1
Low-Pressure Discharges for Plasma Electron Sources

Two conflicting requirements occur in the design of *plasma-cathode* electron sources, both of which need to be met simultaneously. In order to ensure the required *emission current* density, adequate *plasma density* must be attained, for which efficient ionization in the plasma near the *emission boundary* must be provided. On the other hand, accelerating the *electron beam* to the required energy calls for the application of high voltage in the region of electron-beam formation and acceleration; this in turn necessitates decreasing the ionization processes that can cause *breakdown* within the *acceleration gap*. High electric field in the acceleration gap is needed to provide the electron energy, but this same high field can cause breakdown in the gap. This problem can be solved by establishing a pressure difference between the *plasma generation region* and the *electron extraction region*. This is possible, however, only for the case of a relatively small plasma emission surface area, e.g., for small-area focused electron beams. For large-cross-section electron beams or electron beams generated at fore-vacuum pressures, it is difficult or almost impossible to produce such a pressure difference. In this case the choice of an appropriate discharge system that is capable of providing conditions for efficient generation of electrons in the plasma and their stable extraction is likely to be the only way for successful operation of a plasma-cathode electron source.

The discharge employed in plasma-cathode electron sources must provide generation of dense plasma in the region of electron extraction, at the lowest possible pressure. From this standpoint the most suitable kinds of plasma sources are the hollow-cathode glow discharge, discharges in crossed electric and magnetic fields, such as Penning or cylindrical magnetron discharges, the constricted arc discharge, and the vacuum arc. Note that for most plasma cathodes, two different discharge systems are combined into a single device. For instance, one of the discharges (the main discharge) is used to produce the emissive plasma and the other (the auxiliary discharge) is employed to initiate and sustain the main discharge. Let us briefly consider the peculiarities of each of the discharge systems that are most commonly employed in plasma-cathode electron sources.

Plasma Cathode Electron Sources. Efim Oks

ISBN: 3-527-40634-4

1.1 Hollow-Cathode Discharge

The *hollow-cathode discharge* [1] is widely used in various plasma devices, including plasma electron sources. A characteristic feature of this kind of discharge is the oscillation of fast electrons emitted from the inner walls of the cathode cavity and accelerated into the cathode sheath. Unlike reflex discharges in *crossed electric and magnetic fields* where electrons are confined by the magnetic field (see Section 1.2), in the hollow-cathode glow discharge the fast electrons reside within the plasma for a long period of time, being repeatedly reflected in the cathode fall region [2, 3]. There are a number of different hollow-cathode configurations that can provide *electron oscillation*. In plasma electron sources, the *cathode cavity* is normally a hollow cylinder with a central hole in one of its faces (see Fig. 1.1). The characteristic dimensions of the cavity vary from several millimeters to tens of centimeters, depending on the required plasma emission parameters. The optimal ratio of the cavity length l_{cav} to the cavity diameter d_{cav} lies in the range $l_{cav}/d_{cav} \approx 7–10$. The diameter of the hole in the open face of the cavity d_o is typically several times smaller than d_{cav}. *Electrostatic confinement* of electrons in the cathode cavity is responsible for the so-called *hollow-cathode effect*, which shows itself as an abrupt decrease in *discharge operating voltage* and an increase in *discharge current* (see Fig. 1.2), and as an extension of the *operating pressure* range toward lower pressures. Note that the hollow-cathode effect occurs only when the electron mean free path exceeds the characteristic dimensions of the cathode cavity. The type of hollow-cathode discharge is determined by the mechanism of *electron emission* from the cathode surface. In this connection, one can distinguish arc discharges with cold and hot hollow cathodes [4], including a *self-heating* cathode [5, 58, 59], and also high-voltage [6] and low-voltage hollow-cathode glow discharges [12, 57].

A low-voltage discharge with a *"cold" hollow cathode* is rather easily produced; it is characterized by time stability [7] and spatial uniformity [8] of the plasma parameters. This kind of discharge is quite commonly employed for producing

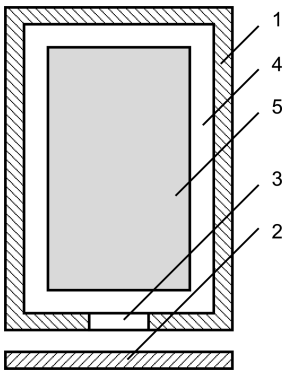

Fig. 1.1 Electrode assembly of the hollow-cathode discharge: 1 – cathode; 2 – anode; 3 – hole; 4 – cathode sheath; 5 – plasma.

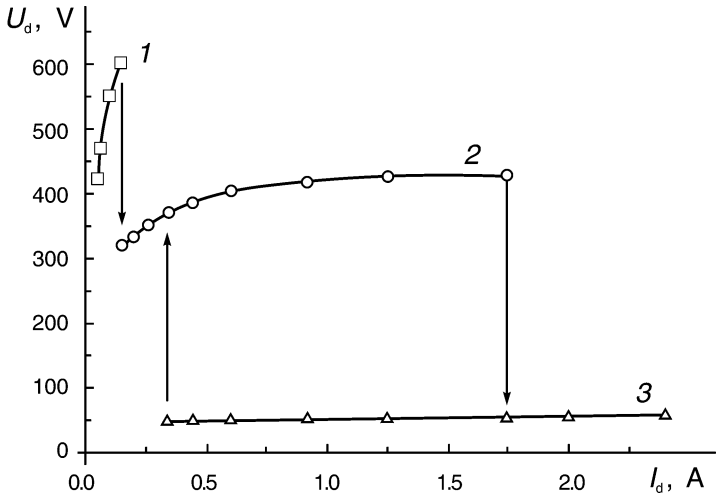

Fig. 1.2 Current–voltage characteristic of the hollow-cathode discharge in different regions of its existence [57]: 1 – glow discharge in the absence of the hollow-cathode effect; 2 – hollow-cathode glow discharge; 3 – cold-cathode arc with cathode spots.

plasmas in plasma-cathode electron sources. Under steady-state conditions, the discharge current I_d in such systems is, as a rule, no greater than 1 A at a discharge operating voltage $U_d = 400$–600 V, yet it can be increased by about an order of magnitude provided that the formation of cathode spots is precluded [9].

In pulsed mode, it is possible to realize a diffuse form of a hollow-cathode discharge in the microsecond range with a current of hundreds of amperes [10]. In this kind of discharge, the plasma electron temperature T_e is generally several electronvolts. The plasma density n_e is determined by the discharge current density to the cathode (from several milliamperes to several amperes per square centimeter) and typically lies in the range $n_e \sim 10^{10}$–10^{13} cm^{-3}.

In studies of the low-voltage hollow-cathode discharge [11], the suggestion was made that *UV radiation* from the *bulk plasma* may result in additional electron emission from the cathode surface. However, the authors [12] came to recognize that *photoelectron emission* can be of only secondary importance. They also suggested that the main factor responsible for the development of the hollow-cathode effect is multiplication of electrons in the cathode potential fall region. The contribution from this factor becomes less significant with increasing discharge current and decreasing operating pressure, when the thickness of the cathode fall region decreases compared to the dimensions of the cathode cavity, and the electron mean free path λ_e becomes much greater than the characteristic width of the discharge gap.

The thickness of the cathode sheath (region of potential fall at the cathode) l_s can be determined by solving simultaneously the well-known *Child-Langmuir* and *Bohm equations* [13]:

$$l_s \approx (\varepsilon_0/n_i)^{1/2}(U_c)^{3/4}/(ekT_e)^{1/4}\,. \tag{1.1}$$

Here e is the electron charge, U_c is the cathode fall potential, n_i is the plasma ion density, and T_e is the electron temperature.

The uniformity of the ion current density distribution over the hollow-cathode surface depends on both the cathode geometry and the operating pressure. In a long and narrow cathode cavity, the plasma density, and hence also the ion current density to the cathode, increases as the exit aperture facing the anode is approached [14]. The discharge system geometry considerably affects the conditions under which the discharge plasma is generated, and consequently the discharge parameters [15, 16]. For efficient oscillation of fast electrons, one should either decrease the exit aperture of the cathode cavity or increase the cathode dimensions. It was shown in [17] that decreasing the ratio of the exit aperture area S_a (in most cases equal to anode area) to the area of the inner surface S_c of the cathode, S_a/S_c, significantly decreases the lower limit to the operating pressure. Moreover, the operating pressure p in this region is directly proportional to S_a/S_c. As S_a/S_c is reduced, the discharge operating voltage rises steeply in response to the decrease in pressure. At a specified operating voltage, the lower limiting pressure and the operating pressure also show an abrupt increase, and a double electrostatic sheath across which $U_s = 10$–40 V is formed in the region of the exit aperture.

Since the cathode cavity is an *electrostatic trap* for *fast electrons* which, oscillating chaotically, can escape only through the exit aperture, the energy of a primary electron expended in ionization depends on the ratio Λ/L. (Here Λ is the relaxation length of the electron: the average distance over which its initial energy decreases to the ionization potential U_i of the working gas, and L is the average distance traversed by an electron inside the cathode cavity before it leaves through the aperture.) For the case where the energy lost by a fast electron is determined only by inelastic collisions with gas molecules, Λ is approximately equal to the *ionization relaxation length* Λ_i, which, according to [17], is estimated as

$$\Lambda_i = (U_c/U_i)\lambda_i\,, \tag{1.2}$$

where λ_i is the mean free path of the electron between two successive ionization events. For $S_a/S_c \ll 1$, the spatial distribution of primary electrons is near-uniform and isotropic. Under these conditions, the S_a/S_c dependence of L can be obtained assuming the oscillating primary electrons to move with equal probability toward all parts of the cathode surface. It has been shown [17] by the use of expressions for the probability of an electron leaving the cavity and for the average length of a single electron transit that

$$L = 4V/S_a\,, \tag{1.3}$$

where V is the volume of the cathode cavity.

For a hollow-cathode glow discharge, the energy of a primary *fast electron* in the operating pressure range is determined by the *cathode fall* potential, which depends on the ratio of the area of the exit aperture to the area of the inner surface of the cathode. The fast electron energy is fully expended in ionization in the cathode cavity only for the case where $\Lambda < L$. At pressures approaching the lower limiting pressure ($\sim 5\times10^{-2}$ Pa), the *electron mean free path* at an energy of 300–600 eV is ~2 m, which is 10–100 times greater than the commonly used cathode cavity diameters. Consequently, the loss of *primary electrons* due to their absorption by the cathode surface does not affect the discharge parameters, whereas electron losses through the exit aperture of the cavity are critical [15–17]. As the exit aperture of the cathode cavity is reduced, an electrostatic *double sheath* may form in the region of the exit aperture where the potential jump is localized. The criterion for the formation of this sheath follows from the equality of the discharge cathode current and anode current [17]. The author of [17] assumed the anode, of rather large surface area, to be negatively charged with respect to the plasma. In this case, the potential difference that results in electron reflection vanishes for $S_a/S_c \approx (m_e/M_i)^{1/2}$. As the ratio S_a/S_c is further decreased, the condition for current passage in the discharge can be fulfilled only if a double sheath with a surface area greater than S_a is formed inside the cathode cavity in the region of the exit aperture. The electrons accelerated in the double sheath are focused and, passing through the (small) exit aperture, ensure equality of the current through the aperture to the anode and the cathode current. Thus the condition for the formation of a double sheath in the region of the exit aperture of the cathode cavity takes the form [17]

$$S_a/S_c < (m_e/M_i)^{1/2}\,. \tag{1.4}$$

Condition (1.4) agrees well with the experimental data for argon reported in [17], where it is demonstrated that with an optimal ratio S_a/S_c a glow discharge can exist in the high-current (2 mA cm^{-2}) low-voltage (below 1000 V) form at pressures of up to 0.03 Pa.

Thus a decrease in S_a/S_c has a beneficial effect on the parameters of the hollow-cathode discharge, involving a decrease in operating voltage and in lower limiting pressure (see Fig. 1.3), only to the point determined by inequality (1.4). Further decrease of this ratio leads to the reverse effect because of the electrostatic double sheath formed in the anode region of the discharge.

For the optimal operating conditions of a hollow-cathode discharge, the lifetime of the electrons is sufficient for them to lose almost all their energy in ionization. Nevertheless, with a magnetic field produced in the cathode region, the discharge operating voltage decreases by 100–150 V [12, 18]. This clearly indicates that the addition of a magnetic field to the hollow-cathode configuration leads to enhanced ionization in the plasma. A drop in discharge operating volt-

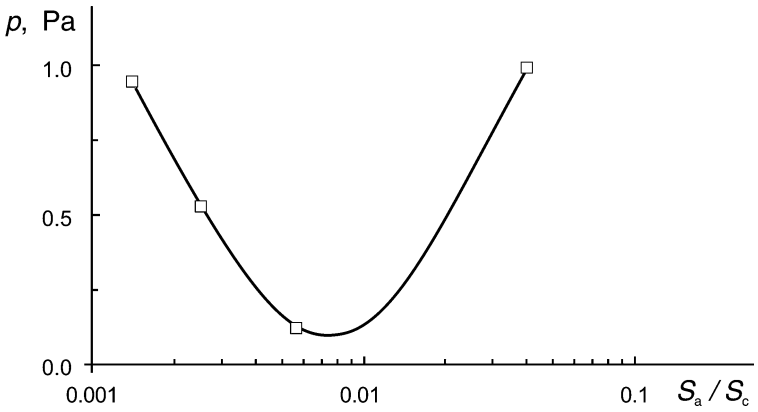

Fig. 1.3 Operating pressure of a hollow-cathode glow discharge versus the ratio of the area of the exit aperture to the area of the inner surface of the cathode [17]. Operating discharge voltage: 600 V.

age in this case is accompanied by fluctuations of the ion current density to a probe. The frequency of these fluctuations lies in the range 5–50 kHz, increasing with increasing magnetic field [18, 19]. The influence of a magnetic field on the operation of a hollow-cathode discharge may be associated with *collective instabilities* arising in the plasma [19]. However, this problem calls for further investigations.

In conclusion, it should be noted that, despite the wide use of the hollow-cathode glow discharge in plasma electron sources, the operating pressure of this type of discharge is somewhat higher than the pressure required for stable electron emission from the plasma. Therefore, a reduction of the operating pressure of a hollow-cathode discharge and its operating voltage is still an urgent problem whose solution is critical for the development of plasma-cathode electron sources based on this kind of discharge.

A number of other aspects of the operation of hollow-cathode discharges as applied to their use in plasma electron sources are considered in [20–23, 43–52].

1.2 Discharges in Crossed Electric and Magnetic Fields

Penning- [24] and *magnetron-type* [25] *discharges* qualify as glow discharges in crossed $E \times B$ fields. These types of discharge are well known and widely employed in various gas discharge devices (ion pumps, gas discharge pressure gauges, ion sources, sputtering systems, etc.). Although the electrode systems of Penning and magnetron discharges are different, the conditions for plasma generation and current passage are so much alike that they can be treated as two kinds of one and the same discharge in a magnetic field. Discharges in crossed

fields, because of electron oscillation, are easily established at low and ultralow pressures and may exist in the high-current, low-voltage form in the operating pressure ranges of plasma electron sources, affording the required electron-beam current. It is significant that, in plasma electron emitters based on discharges in crossed $E \times B$ fields, no problem arises in matching the cathode and the external magnetic field, which can be used to focus and/or transport the accelerated electron beam.

Simple schematics of the electrode systems of Penning and magnetron discharges are shown in Fig. 1.4a and b, respectively. The electrons accelerated in the cathode fall region are confined by the magnetic field, moving in crossed $E \times B$ fields along closed trajectories, reciprocally in a Penning discharge and along a cycloid path in a magnetron discharge. Fast electrons can escape from the discharge system and reach the anode only when almost all their energy is lost in repeated collisions. These conditions provide a high *degree of ionization* of the working gas up to a gas pressure of 10^{-2} Pa, which is somewhat lower than the pressure required for a hollow-cathode glow discharge.

Interest in magnetron-type discharges with cylindrical electrodes (see Fig. 1.4b) stems from the feasibility of a *tubular* (otherwise termed "annular") *electron-beam* source. Such an electrode system, if used in an *inverted magnetron* type of configuration (anode 2 inside cathode 1 and facing electrodes 3 at cathode potential), ensures more efficient electron confinement. Experiments with plasma-cathode electron sources have shown that over the operating pressure range an ignition voltage $U_{ig} = 1.5$–2.0 kV and a magnetic field $B \approx 0.01$ T are sufficient for stable initiation of a discharge in the "inverted magnetron" system [26]. The discharge operating voltage falls within $U_d = 400$–600 V and the current slowly increases with discharge voltage.

In plasma-cathode electron sources, the maximum *electron emission current* depends on the discharge current reached. The maximum current in a magnetron discharge, I_{dmax}, is limited by the formation of cathode spots and by the *discharge-to-arc transition*. The value of I_{dmax} is determined in many respects by the working gas pressure and the kind of gas, by the condition and area of the surface, and in pulsed mode by the discharge pulse duration. With helium, the discharge current in the diffuse mode can reach $I_{dmax} = 1.2$ kA for a discharge current pulse duration $\tau_d = 20$ μs and a current density to the cathode $j_{dmax} = 5$ A cm^{-2} [27]. The decrease in I_{dmax} with increasing discharge current pulse duration τ_d is described to reasonable accuracy by the empirical relation [28]

$$I_{dmax} = A/\tau_d^{2/3} . \tag{1.5}$$

The electron temperature measured in the discharge is $T_e = 4$–8 eV and the plasma density lies in the range $n_e = 10^{10}$–10^{13} cm^{-3}, depending on the discharge current.

A number of other aspects of the operation of discharges in crossed $E \times B$ fields applied to its use in plasma electron sources are considered in [44, 46, 53–56].

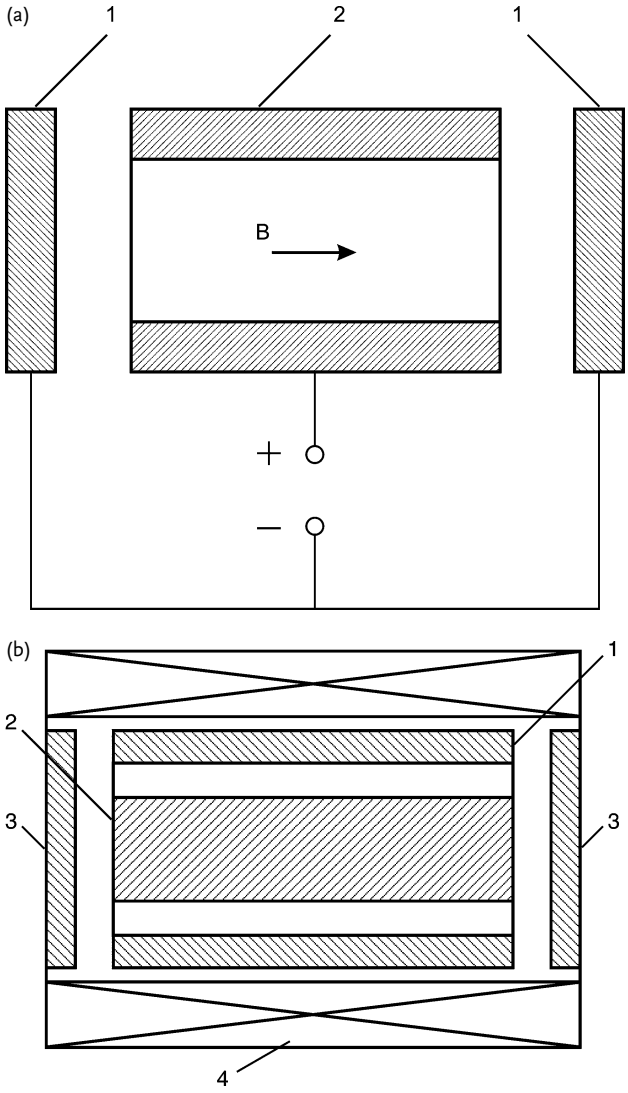

Fig. 1.4 (a) Electrode system of a Penning-type discharge: 1 – flat cathodes; 2 – cylindrical anode. (b) Electrode system of a cylindrical magnetron-type discharge: 1 – cathode; 2 – anode; 3 – facing electrodes; 4 – solenoid.

1.3
Arc Discharges

In plasma-cathode electron sources, the beam current is comparable to the discharge current at which the plasma is generated. Therefore, an increase in emission current necessitates a corresponding increase in discharge current. In a glow discharge, the discharge current density and the total discharge current are limited to a value which approximates the minimum current for formation and stable operation of *cathode spots*. The current in the diffuse kind of glow discharge can be increased by increasing the *cathode surface area*. In so doing, it is worthwhile to limit the cathode current so that the current density is lower than that at which cathode spots are formed. This approach is important when specific electron-beam parameters are required. However, this does not resolve the fundamental problem of limiting the discharge current and the emission current in plasma electron sources utilizing glow discharges.

The quest for higher electron-beam current and electron-beam density has generated a need to employ *arc-type discharges* in plasma electron sources. In the absence of *hot thermionic electrodes* (for maximum advantage of the plasma electron gun it should not contain any electrodes heated up to thermionic emission temperature), the arc discharge is characterized by one or several cathode spots operating on the negative electrode. The cathode spot of an arc discharge exhibits "unlimited" emissivity, allowing electron beams with extremely high specific and average parameters. Plasma electron sources make use of two forms of the arc discharge: a *vacuum arc* where the emissive plasma is produced directly from the cathode spot, and a *constricted low-pressure arc* discharge where the cathode spot is shielded from the region of electron extraction by an *electrostatic double sheath* and the emission plasma is generated as a result of residual gas ionization by electrons.

1.3.1
Vacuum-Arc Discharge

A schematic of a vacuum-arc discharge system that can be used for generating electron beams is shown in Fig. 1.5. The vacuum arc is a discharge between two electrodes in which the plasma-forming medium is provided by the electrode material evaporated at one or several cathode spots. These cathode spots and the current transfer that they provide at the cathode are inherent to vacuum arcs, distinguishing this type of discharge from other arc discharges.

The cathode spot is a micron-sized intense plasma region that moves over the electrode surface, drawing a discharge (cathode) current of density $j_d \approx 10^6$–10^8 A cm^{-2}. With such a high discharge current density, local surface heating of the electrode material causes its evaporation within the cathode spot region and a dense metal plasma is generated that expands toward the anode at a speed $v_i \sim 10^4$ m s^{-1}. The density of the *expanding plasma* decreases with distance from the cathode spot as a near inverse square law, typically reaching $n_e \approx 10^{10}$–

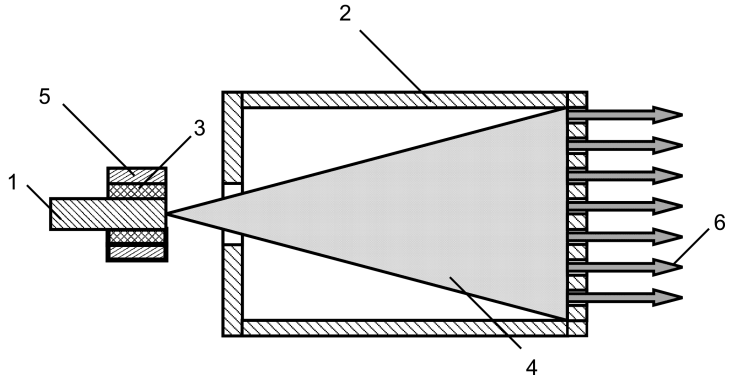

Fig. 1.5 Electrode assembly of the discharge system of a plasma electron source based on a vacuum arc: 1 – cathode; 2 – anode; 3 – ceramic ring; 4 – plasma flux; 5 – trigger electrode; 6 – electron beam.

10^{12} cm^{-3} in the electron extraction region. The processes occurring in the cathode spot and their influence on current transfer and on the plasma parameters are critical features of a vacuum-arc discharge. Cathode spots are unstable; they move chaotically over the cathode surface, governing the nonuniformity of the plasma density and plasma instability, which finally affect the quality of the extracted electron beam. The existence of cathode spots leads to *erosion of the cathode* material. All the processes responsible for the erosion take place in a *surface sheath* about 1–2 μm thick. The sputtering rate of the electrode material is typically of order 10^{-5} g per coulomb of charge transferred in the arc. There are two kinds of cathode spots. *Cathode spots of the first kind* arise at the initial moments of the discharge when dielectric films and gaseous inclusions are present on the cathode surface. Such spots move rapidly over the cathode, resulting in moderate erosion of its surface. *Cathode spots of the second kind* are much larger and their velocity is much slower compared to cathode spots of the first kind. They are formed after hundreds of microseconds after arc ignition, for arc currents of hundreds of amperes. Such spots invariably occur on well-cleaned and decontaminated cathode surfaces.

An important feature of the cathode spot is its *cyclic operation*. A cathode spot changes its potential and other parameters every cycle, whose duration for most metals is of order 10^{-8} s. The lifetime of an individual spot (between its formation and extinction) spans a great number of cycles, yet it is normally no longer than a few microseconds.

A cathode spot requires a *minimum current* to exist. The threshold current at which a cathode spot is formed is determined by the electrode material and the state of its surface. For pure metals, the threshold current lies in the range from hundreds of milliamperes (zinc) to several amperes (nickel). In pulsed mode, the threshold current increases and can reach tens of amperes even in the microsecond range.

The plasma of a vacuum-arc discharge contains a large fraction of *multiply charged ions*. The *average ion charge state* $\langle Q_i \rangle$ can be greater than 2+, with ions of charge states $Q_i = 2+$ to 5+ present in the plasma, depending on the cathode material. In a strong magnetic field, the average ion charge state nearly doubles and the ion drift energy, corresponding to the directed ion velocity v_i, is several times greater than both the cathode fall potential and the voltage drop across the whole electrode gap. The *direct velocities of ions* of different charge states are nearly equal [29].

For a vacuum-arc discharge, the *breakdown voltage* of the gap is orders of magnitude greater than the steady-state operating voltage. In this connection, the initiation of an arc at comparatively low voltages applied across the gap is important. In vacuum-arc ion and electron sources, the discharge normally operates in a repetitively pulsed mode, with a discharge current pulse duration ranging from tens to hundreds of microseconds. The *pulse repetition rate* can thus be the same as the mains supply line frequency (50 or 60 Hz). Among a variety of methods of vacuum-arc initiation, the formation of a cathode spot at the electrode contacting the plasma, and a *glow-to-arc transition* method, most fully satisfy the condition for arc initiation in repetitively pulsed mode. In this case, cathode spots are due to charging of dielectric films and inclusions on the electrode surface by the ion flux from the plasma and their subsequent breakdown.

For the most part the "plasma method" of triggering is accomplished by using a *surface discharge*. The principle of this procedure is illustrated in Fig. 1.6. Vacuum-arc cathode 1 and trigger electrode 7 are 1–2 mm apart with ceramic insulator 8 between them. A high-voltage pulse of several kilovolts and duration of order 10 μs is applied between the electrodes 1 and 7. A sliding surface discharge thus initiated produces dense plasma near the cathode. Ions

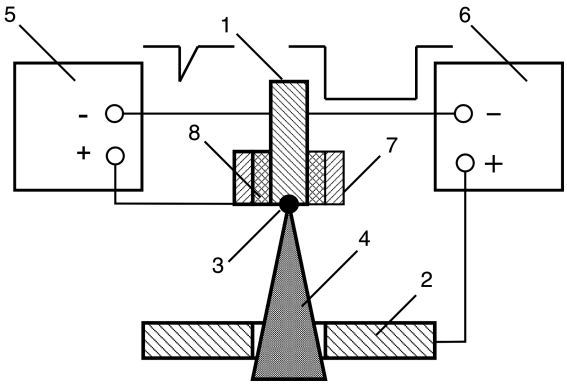

Fig. 1.6 Electrode system for vacuum-arc triggering by flashover discharge: 1 – cathode; 2 – anode; 3 – cathode spot; 4 – plasma flux; 5 – power supply for the triggering discharge; 6 – power supply for the vacuum arc; 7 – trigger electrode; 8 – ceramic ring.

from this plasma bombard the cathode and initiate a cathode spot at its surface, normally at the *metal–dielectric contact* region. Since the discharge current to the *trigger electrode* is limited by the resistance of the secondary winding of the pulse transformer of power supply 5, the discharge switches to anode 2, giving rise to a vacuum arc between the cathode 1 and the anode 2. This method of vacuum-arc initiation by an auxiliary surface discharge is rather simple and reliable, and provides small delay times. However, the lifetime of this kind of triggering system is no greater than 10^5–10^6 pulses, and ions from the sputtered dielectric and trigger electrode materials are found in the arc plasma.

The use of a glow-to-arc transition for initiating the first vacuum-arc cathode spot (i.e., for triggering the vacuum-arc discharge) calls for the efficient ignition and stable operation of an *auxiliary glow discharge* at very low pressure. Dis-

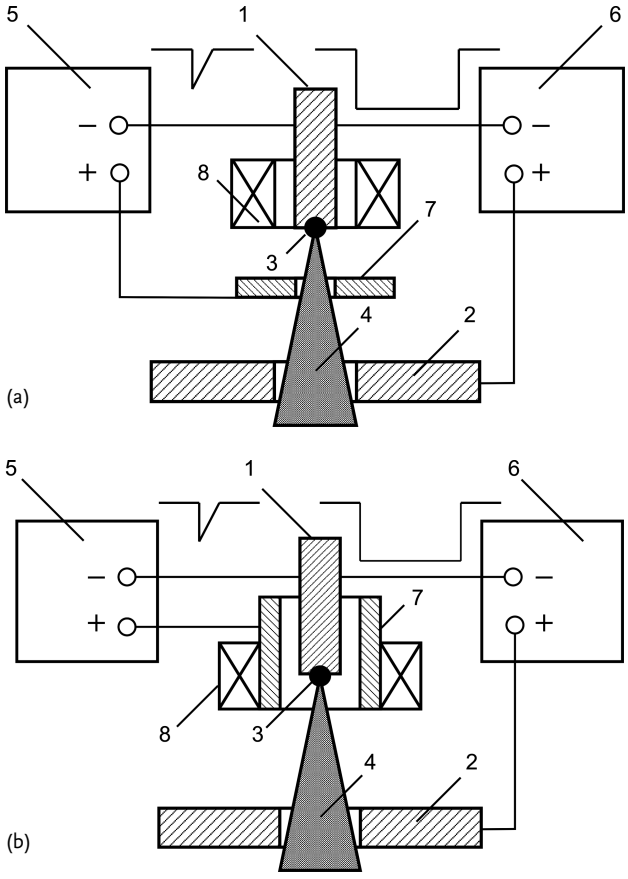

Fig. 1.7 Electrode systems of (a) vacuum-arc triggering by an auxiliary Penning discharge and (b) vacuum-arc initiation by an auxiliary magnetron discharge: 1 – cathode; 2 – anode; 3 – cathode spot; 4 – plasma flux; 5 – power supply for the triggering discharge; 6 – power supply for the vacuum arc; 7 – trigger electrode; 8 – solenoid.

charges in crossed electric and magnetic fields ($E \times B$), such as Penning or cylindrical magnetron discharges, satisfy these requirements well. In discharges of this type, oscillating electrons are confined within the cathode–anode gap, and thus these plasmas are rather easily formed at low pressures, down to high vacuum, and can provide an ion current sufficient for a cathode spot to form at the electrode surface. Schematics of systems based on auxiliary discharges in $E \times B$ fields are presented in Fig. 1.7 a (Penning discharge) and Fig. 1.7 b (cylindrical magnetron discharge).

These methods of vacuum-arc triggering are highly reliable and efficient. Their lifetime is greater than 10^7 pulses. However, such systems are rather complicated. They require special electrodes and magnetic field that add complexity to both the plasma electron source and its power supplies.

More detailed information on the processes occurring in vacuum-arc discharges and on the current status of research on the physical processes in the vacuum-arc cathode spots can be found in [30–32, 42]. A critical analysis of methods of vacuum-arc initiation is given in [33].

1.3.2 Constricted Low-Pressure Arc Discharge

The constricted positive column of a low-pressure arc discharge is employed in "duoplasmatron" and "duopigatron" ion sources [41] and in a number of high-current switching devices [42]. Constriction is aimed mainly to increase the local plasma density in the discharge constriction region. In plasma electron sources, the use of a *constricted arc* also allows the required pressure difference between the discharge region and the region of electron extraction and acceleration. This provides stable ignition and operation of the discharge and also a high electric field strength at the acceleration gap. When used in discharge systems free of hot electrodes, as is common for plasma-cathode electron sources, constriction of an arc discharge makes it possible to eliminate or significantly reduce the dependence of the plasma parameters in the electron extraction region on instabilities of the plasma and the discharge parameters associated with cathode spots.

The general features of the constricted arc discharge are comprehensively described in [34]. Arc discharges are most often constricted by a hole or a channel (of diameter and length 2–6 mm) in an intermediate electrode that is at floating potential (see Fig. 1.8). The electrode configuration of the constricted arc discharge system and the distributions of potential and particle density near the electrostatic double-charged sheath are shown in Fig. 1.9. A characteristic feature of this type of discharge is the stationary *double sheath* present at the inlet of the constriction channel. This double sheath focuses and accelerates the electrons arriving in the *constriction channel*. Formation of the double sheath is due to an abrupt increase in plasma density in the constriction channel (by 1–3 orders of magnitude compared to the plasma density upstream of the channel) and to the increased number of ions lost to the channel walls by radial diffusion.

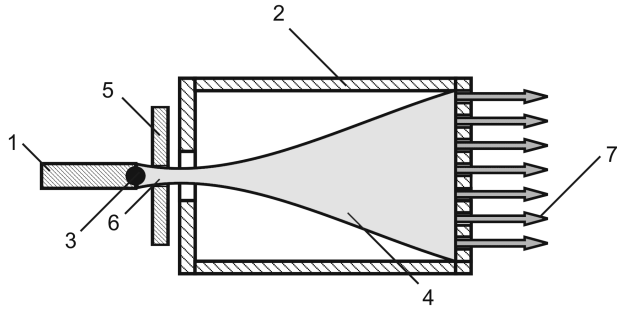

Fig. 1.8 Electrode assembly of the discharge system of a plasma electron source based on a constricted arc discharge: 1 – cathode; 2 – anode; 3 – cathode spot; 4 – plasma flux; 5 – intermediate electrode; 6 – constriction channel; 7 – electron beam.

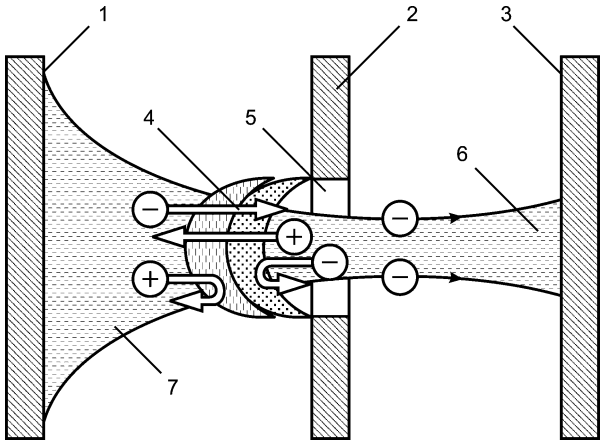

Fig. 1.9 Electrode system for the constricted arc discharge: 1 – cathode; 2 – intermediate electrode; 3 – anode; 4 – double sheath; 5 – constriction channel; 6 – anode plasma; 7 – cathode plasma.

Assuming that the electric field strength on either side of the sheath and the initial velocities of the electrons and ions arriving in the sheath from the cathode and anode regions are zero, and neglecting the reverse flow of electrons that have overcome the *potential barrier*, we obtain that the ratio between the electron current density j_e and ion current density j_i in the double sheath is approximately proportional to the square root of the ion–electron mass ratio:

$$j_e/j_i \cong (M_i/m_e)^{1/2} . \tag{1.6}$$

On the assumption that the plasma electron temperatures T_e on both sides of the double sheath are equal, the voltage drop across the double sheath U_s can be estimated as

$$U_s \cong (kT_e/e)\ln(n_1/n_2)\,. \tag{1.7}$$

Here n_1 and n_2 are the plasma densities in the constriction channel and in the cathode region, respectively. The voltage drop across the double sheath can lie in the range $U_s = 20$–120 V, depending on the constriction channel geometry and the discharge parameters.

The electrons accelerated in the double sheath display a high ionizing capacity. Hence, the current at the outlet of the constriction channel is the current of two groups of electrons. One consists of fast electrons that have passed through the double sheath and the constriction channel without any interaction and energy loss, and the other consists of slow electrons resulting from ionization of the gas by fast electrons.

In a constricted arc discharge, electrons are extracted from the *expanded plasma surface* in the discharge anode region. The plasma electrons resulting from relaxation of fast electrons by their collective interaction with the anode plasma make a major contribution to the generation of the anode plasma of a constricted discharge [35].

The anode cavity of a constricted arc discharge in a plasma electron source is typically a cylinder whose diameter is approximately equal to its length and is about 10 cm. Results of detailed investigations of the constricted arc discharge with extended anode section as used in plasma electron sources, including theoretical analysis and numerical simulation of the ionization processes in the discharge anode region and experimental studies of the plasma and discharge parameters, are reported in [35].

Experimental studies of electron emission from the plasma of a low-pressure arc discharge have been carried out using a plasma cathode based on a constricted arc discharge with extended anode section (see Fig. 1.10). The pulsed arc discharge ($I_d = 50$–200 A, $\tau_d = 100$ μs) between cold cathode 1 and cylindrical hollow anode 4 (radius $r_a = 5$ cm and length $l_a = 10$ cm) was constricted with a hole made in an intermediate electrode 2 (see Fig. 1.10). In so doing, at the inlet of the constriction hole an electrostatic double sheath was formed in which the electrons from the cathode region were accelerated. The anode face was covered with fine metal grid 5, which stabilized the plasma emission boundary. The accelerating electrode (collector) 6 was placed 1 cm away from the grid plane. The wide aperture of the emitting electrode did not allow a pressure difference between the regions of plasma generation (the anode cavity) and electron extraction (the acceleration gap). The pressure in these regions was varied over 10^{-4}–10^{-3} Torr by changing the flow rate of the working gas (argon, nitrogen).

With the plasma and discharge parameters obtained in this device, the thickness of the *near-anode sheath* l_s was in the range 0.3–3 mm. The size of the elementary grid mesh h was chosen to be 0.1–3 mm so that electrons could be ex-

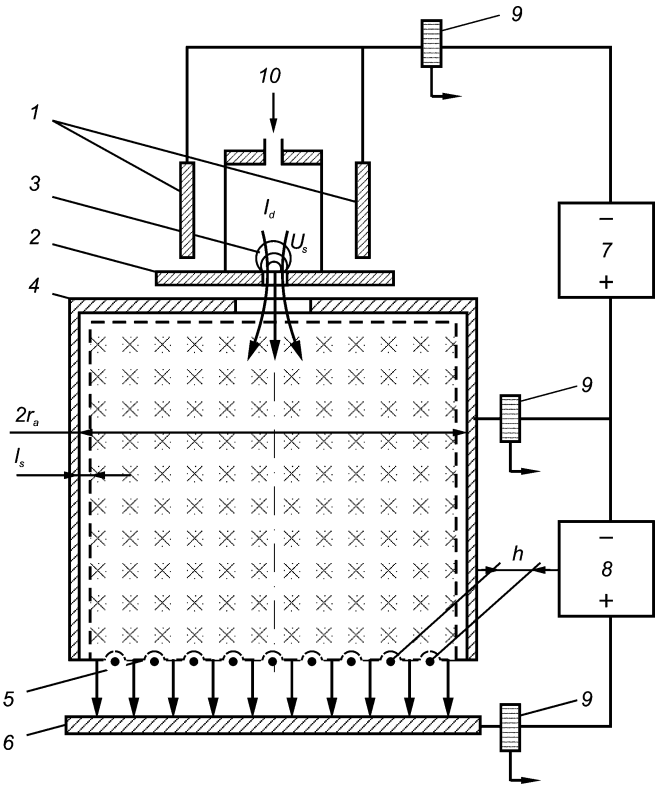

Fig. 1.10 Electrode assembly of a plasma electron emitter based on a constricted arc discharge: 1 – cathode; 2 – intermediate electrode; 3 – double layer; 4 – hollow anode; 5 – grid; 6 – collector; 7 – power supply for the discharge; 8 – accelerating voltage source; 9 – Rogowskii coil (current transformer); 10 – working gas input.

tracted from the plasma in three different regimes: emission from the open plasma surface ($h \gg 2l_s$), emission through the potential barrier ($h \ll 2l_s$), and also an intermediate mode in which electrons are emitted from the partially open plasma surface ($h \approx 2l_s$).

The plasma parameters were measured with single Langmuir, double, and emissive probes. The *electron energy distribution* in the plasma was studied with an electrostatic (retarding grid) energy analyzer.

Measurements of the *electron energy* at the anode cavity inlet have shown that the electron current in this region is mainly from fast electrons accelerated in the double sheath of the constriction channel. At the same time, at a distance of about 10 cm from the inlet the electron component of the discharge current at the emission face and at the side walls of the anode cavity consists mainly of relatively slow plasma electrons. These electrons do not result from ionization of the gas, since the percentage of these particles, estimated by measuring the total ion current at the anode walls, is no greater than 5% of the electron current at the cavity.

The percentage of fast electrons at the anode walls is no more than 15% of the electron current in the cavity. The abrupt decrease in the percentage of fast electrons in their passage through the anode cavity cannot be due to secondary electron production in the gas, since under these experimental conditions the electron mean free path was much greater than the characteristic dimensions of the cavity. The relaxation of the beam is presumably associated with collective processes within the cavity.

Experiments have shown that in a low-pressure arc discharge with extended anode section the plasma parameters are unaffected by the way in which the discharge is initiated and by the details of the electrode system. This makes it possible to consider in one and the same context the physical processes occurring in plasma sources for large-cross-section electron beams. Our physical model of the plasma cathode using this type of discharge allows a description of the processes involved, including some general features of plasma formation when plasma electrons are extracted. In this model, the homogeneous electron beam is accelerated in the cathode potential fall region U_c or in the double sheath by a voltage U_s and streams to the anode cavity. Residual gas ionization in the anode cavity forms plasma there that is separated from the anode walls by an ion sheath, which is actually a potential barrier for plasma electrons. The energy of fast electrons is lost in their interaction with the plasma. The resulting low-energy electrons also ionize the gas. Moreover, secondary electrons knocked out of the cavity walls and accelerated in the anode sheath can also contribute to ionization. In this discharge system, the bottom end surface of the hollow anode is covered with an electrode with holes of radius r_0 through which electrons are emitted from the plasma. The plasma parameters are determined from the equations of ion balance, energy balance, current continuity, and plasma charge neutrality. Taking into account the possible electron emission, the system of *balance equations* takes the form

$$
\begin{aligned}
&I_d q_1 L_1 + I_\sigma q_2 L_2 + A N_e k T_e (U_i + 2kT_e) \exp(-U_i/kT_e) = I_i/N_0 \,, \\
&I_d = I_f + I_\sigma + I_e + I_i + I_{em} \,, \\
&I_d U_s \{1 - \exp[(L_1 - 1)/L_1]\} + I_\sigma \varphi_\sigma \{1 - \exp[(L_2 - 1)/L_2)]\} \\
&\qquad = 2kT_e (I_e + I_{em}) + I_i (U_i + \varphi_{pl}), \\
&N_i = N_e + C I_c L_1 / (U_s + \varphi_{pl})^{1/2} + C I_\sigma L_2 / (\varphi_\sigma + \varphi_{pl})^{1/2} \,.
\end{aligned}
\tag{1.8}
$$

Here I_d is the discharge current; I_f, I_σ, I_e, I_i, and I_{em} are, respectively, the anode components of the current of fast, secondary, and plasma electrons, the ion current to the anode, and the current of plasma electron emission; q_1 and q_2 are the ionization cross-sections for fast and secondary electrons; L_1 and L_2 are the free paths of fast and secondary electrons that are divided to the anode cavity length; N_i and N_e are, respectively, the number of ions and electrons per unit length of the anode cavity; eU_s and $e\varphi_\sigma$ are the energy of fast electrons and the initial energy of secondary electrons; φ_{pl} is the potential of the plasma with re-

spect to the anode; N_0 is the number of neutrals per unit cross-sectional area of the positive discharge column; $C=(m_e/2e^3)^{1/2}$; $A=a_i(8k^3/\pi m_e)^{1/2}$; and a_i is a coefficient dependent on the gas species.

The system of balance equations (1.8) has been solved numerically for the external discharge parameters typical for plasma electron sources. The results of the calculations agree satisfactorily with experiment. Measurements and calculations for the discharge operation without electron extraction have shown the electron temperature in the plasma T_e to be 5–10 eV, depending only slightly on the discharge current and decreasing considerably with increasing pressure (see Fig. 1.11). This dependence may be associated with an increase in the rate of electron interaction with ions and neutral particles and, consequently, with a more intense energy exchange between the plasma particles. Both calculations and experiment show that the plasma density $n_e=10^{10}$–10^{11} cm^{-3}. In the low-pressure range, a more drastic increase in n_e is observed with increasing p (see Fig. 1.12). With no electron emission, the plasma potential φ_{pl} exceeds the anode potential by several volts. The dependence $\varphi_{pl}(p)$ has a maximum. As the discharge current is increased, the position of the maximum shifts toward lower pressures. The nonmonotonic character of $\varphi_{pl}(p)$ may be due to the combined effects of n_e and T_e, which

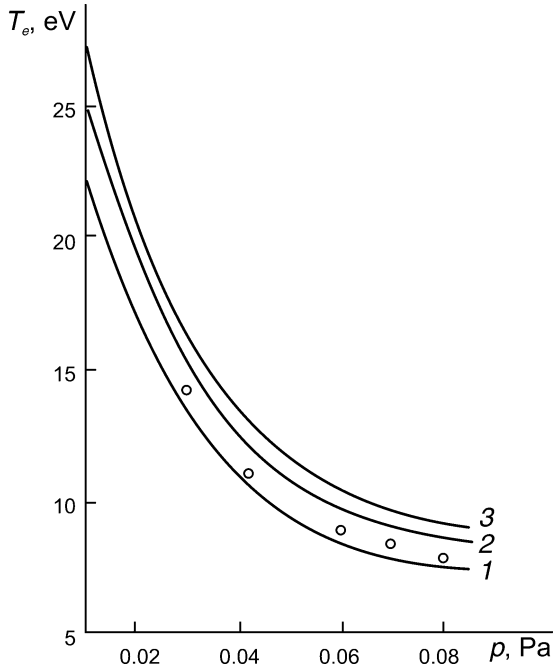

Fig. 1.11 Calculated dependences of the plasma electron temperature on argon pressure for the following voltages across the double sheath U_s and discharge currents I_d: curve 1 – 30 V, 5 A; curve 2 – 100 V, 5 A; curve 3 – 100 V, 100 A. Circles – experiment ($I_c=20$ A).

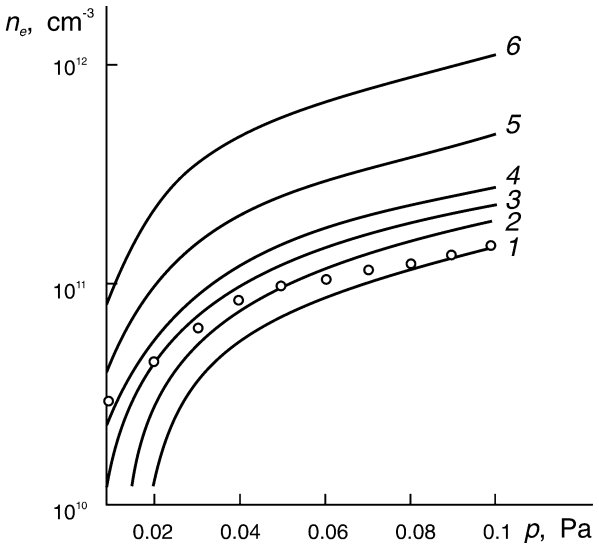

Fig. 1.12 Calculated dependence of the plasma electron density on the nitrogen pressure at the following voltages across the double sheath U_s and discharge currents I_d: curve 1 – 40 V, 15 A; curve 2 – 60 V, 15 A; curve 3 – 80 V, 15 A; curve 4 – 100 V, 15 A; curve 5 – 100 V, 40 A; curve 6 – 100 V, 60 A. Circles – experiment (I_d=40 A).

are responsible for the steady-state value of φ_{pl}. The increase of electron temperature as well as of plasma density defines the increase in plasma potential. However, as can be seen in Figs. 1.11 and 1.12, these parameters respond to a pressure buildup in various ways and the dependence $\varphi_{pl}(p)$ is governed by the predominant action of one or the other of these factors.

The electron temperature T_e varies with the anode cavity geometry via the ratio of the surface area of the hollow anode S_a to its volume V_a. This influence of geometry on T_e is due to the fact that, under the discharge operating conditions in question, ionization is mainly by plasma electrons. A peculiar feature of the dependence $T_e(S_a/V_a)$ is its near-linear character, with a slope dependent on the gas pressure in the cavity [36].

In a constricted arc discharge, shielding of the cathode spots by the double sheath provides rather stable parameters of the anode plasma and thus a high quality of the electron beam extracted from the plasma. However, the discharge current in the constriction channel is limited. With a discharge current in excess of some limiting value I_{dmax}, fluctuations and cutoffs of the arc current are observed. As indicated in [34], discharge instability is caused by a decrease in neutral density in the constriction channel, since the directed impulse transmitted to the neutrals in their elastic collisions with electrons carries them out of the constriction channel. Under steady-state discharge conditions, the value of I_{dmax} is determined by the area of the constriction channel S, the initial pressure of the working gas p_0, the kind of gas, and the flow rate in the constricted channel Q:

$$I_{\mathrm{dmax}} = eQ(M_{\mathrm{i}}/m)^{1/2}(\sigma_{\mathrm{imax}}/\sigma_{\mathrm{e0}})/(1+a) \approx Ap_0S\,. \tag{1.9}$$

Here σ_{imax} is the maximum ionization cross-section of the gas by electron impact; σ_{e0} is the elastic collision cross-section for electrons with neutral molecules; and a is a dimensionless parameter which takes into account the ion loss to the channel walls and is determined by the ratio between the ion current at the channel walls and the ion current to the double sheath.

In pulsed mode when the gas pressure in the channel is unsteady, the maximum stable discharge current is about an order of magnitude higher than for steady-state gas pressure. However, this current decreases rapidly with increasing pulse duration and pulse repetition rate. Experiments show that the characteristic time in which the gas pressure in the constriction channel and thus I_{dmax} takes on a steady-state value is tens of microseconds.

Increasing the current to more than I_{dmax} causes fluctuations and cutoffs of the discharge current. However, a further increase in current after cutoff may lead to stable operation of the discharge over a wide range of amplitude and duration of the discharge current pulse. The steady-state current observed in this case is due to a transition of the discharge to the so-called *cascade mode,* in which cathode spots are formed on the intermediate electrode surface facing the anode. The constricted discharge is divided into two arcs operating one after the other. The arcs have a common discharge current, but each of them is sustained by its own cathode spots. In essence, a vacuum-arc discharge capable of stable operation even after the extinction of the first cascade is ignited between the intermediate electrode and the anode. The cascade operation of the arc can be precluded or even eliminated if the constriction channel is made in the form of several insulated thin metal sections.

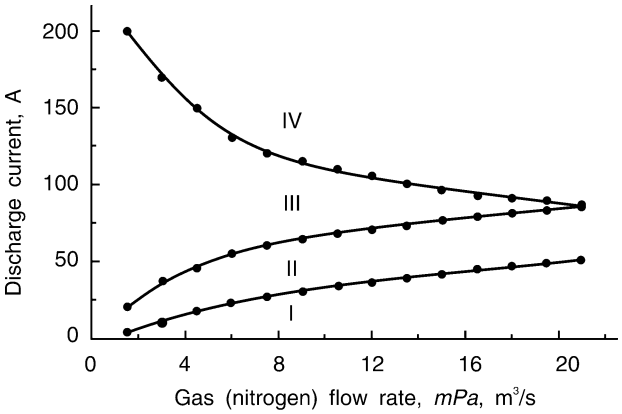

Fig. 1.13 Operating modes of the constricted arc discharge. Pulse duration 50 μs, pulse repetition rate 50 Hz: region I – stable operation of the constricted arc discharge; II – fluctuations and cutoffs of the discharge current; III – "cascade" arc; IV – "self-pinched" discharge.

However, here too the constricted arc discharge regains stability after unstable operation, but at higher discharge currents. This is associated with confinement of the arc in the constriction channel by its self-magnetic field (the so-called *self-pinch effect*). The range of stable operation of the constricted arc discharge in different modes is shown in Fig. 1.13. Note that presently available plasma-cathode electron sources employ only an "ordinary" constricted arc discharge (region I, Fig. 1.13), and also the cascade mode of operation (region III, Fig. 1.13), which is essentially a vacuum arc. The results of detailed studies of the operating modes of constricted low-pressure arc discharges have been reported in [37–40].

References

1 B. I. Moskalev, *Hollow-Cathode Discharges* (Energia, Moscow, 1969) (in Russian).
2 A. S. Metel, A. I. Nastyukha, Izvestiya Vysshikh Uchebnykh Zavedenii, Radiofizika, **19**, No. 12, 1891 (1976). Translated in: Radiophysics and Quantum Electronics.
3 A. S. Metel, A. I. Nastyukha, Izvestiya Vysshikh Uchebnykh Zavedenii, Radiofizika, **19**, No. 12, 1078 (1976). Translated in: Radiophysics and Quantum Electronics.
4 D. P. Borisov, N. N. Koval, P. M. Schanin, Russian Physics Journal, **37**, No. 3, 295 (1994).
5 A. Hershcovitch, V. J. Kovaric, K. Prelec, Journal of Applied Physics, **67**, No. 2, 671 (1990).
6 J. J. Rocca, M. R. Meyer, M. R. Farrell, Journal of Applied Physics, **56**, No. 3, 790 (1984).
7 D. M. Goebel, A. T. Forrester, Review of Scientific Instruments, **53**, No. 6, 810 (1982).
8 V. G. Grechanyi, A. S. Metel, High Temperature, **22**, No. 3, 355 (1984).
9 A. V. Vizir, E. M. Oks, M. V. Shandrikov, G. Yu. Yushkov, Instruments and Experimental Techniques, **46**, No. 3, 384 (2003).
10 D. M. Goebel, R. M. Watkins, Review of Scientific Instruments, **71**, No. 2, 388 (2000).
11 V. A. Gruzdev, Yu. E. Kreindel, G. G. Vasylyeva, *Proceedings of the 10th International Conference on Phenomena in Ionized Gases* (Donald Parsons, Oxford, 1971), Part 1, p. 111.
12 V. N. Glazunov, A. S. Metel, Soviet Physics – Technical Physics, **26**, No. 5, 559 (1981).
13 M. A. Lieberman, "Fundamentals of plasmas and sheaths", in *Handbook of Plasma Immersion Implantation and Deposition*, ed. A. Anders (John Wiley and Sons, New York, 2000), Ch. 2.
14 M. Yu. Kreindel, I. V. Osipov, N. G. Rempe, Soviet Physics – Technical Physics, **37**, No. 10, 1046 (1992).
15 V. G. Grechanyi, A. S. Metel, Soviet Physics – Technical Physics, **27**, No. 3, 284 (1982).
16 V. N. Glazunov, A. S. Metel, Physics of Plasmas, **8**, No. 5, 1099 (1982). Translated in: Soviet Journal of Plasma Physics.
17 A. S. Metel, Soviet Physics – Technical Physics, **29**, No. 2, 141 (1984).
18 E. M. Oks, A. Anders, I. G. Brown, Review of Scientific Instruments, **75**, No. 4, 1030 (2004).
19 E. M. Oks, A. Anders, I. G. Brown, et al., Plasma Physics Reports, **31**, No. 11, 978 (2005).
20 Yu. E. Kreindel, S. P. Nikulin, Soviet Physics – Technical Physics, **33**, No. 6, 714 (1988).
21 G. I. Kirichenko, V. M. Tkachenko, V. B. Tyutyunnik, Soviet Physics – Technical Physics, **21**, No. 9, 1080 (1976).
22 V. A. Burdovitsin, M. F. Repin, Soviet Physics Journal, **33**, No. 4, 336 (1990).
23 A. V. Zharinov, Yu. A. Kovalenko, Russian Physics Journal, **44**, No. 9, 947 (2001).
24 F. M. Penning, "Coating by cathode disintegration", US Patent 2146025, N. V. Philips, Eindhoven, The Netherlands (1939).

25 N. A. Kervalishvili, A. V. Zharinov, Soviet Physics – Technical Physics, **10**, No. 12, 2194 (1965).

26 E. M. Oks, A. A. Chagin, Soviet Physics – Technical Physics, **33**, No. 6, 702 (1988).

27 E. M. Oks, A. A. Chagin, P. M. Schanin, *Proceedings of the First All-Union Conference on Plasma Emission Electronics* (Buryat Scientific Center, Ulan-Ude, 1991), p. 18 (in Russian).

28 A. V. Kozyrev, E. M. Oks, A. A. Chagin, *Proceedings of 20th International Conference on Phenomena in Ionized Gases* (Pisa, Italy, 1991), Vol. 2, p. 498.

29 G. Yu. Yushkov, A. S. Bugaev, I. A. Krinberg, E. M. Oks, Doklady Physics, **46**, No. 5, 307 (2001).

30 G. A. Mesyats, *Ectons in a Vacuum Discharge: Breakdown, Spark, Arc* (Nauka, Moscow, 2000) (in Russian).

31 S. M. Shkolnik, K. W. Struve (eds.), IEEE Transactions on Plasma Science, **33**, No. 5, part 1 (2005), Special Issue on vacuum arc plasmas.

32 B. Juttner, Journal of Physics D: Applied Physics, **34**, 103 (2001).

33 A. Anders, I. G. Brown, R. A. MacGill, M. R. Dickinson, Journal of Physics D: Applied Physics, **31**, 584 (1998).

34 V. L. Granovskii, *Electric Current in Gases: Steady-State Current* (Nauka, Moscow, 1972) (in Russian).

35 V. L. Galanskii, Yu. E. Kreindel, E. M. Oks, et al., High Temperature, **25**, No. 5, 632 (1987).

36 V. L. Galanskii, Yu. E. Kreindel, E. M. Oks, A.G. Ripp, High Temperature, **27**, No. 2, 390 (1989).

37 N. N. Koval, N. P. Kondrat'eva, Yu. E. Kreindel, P. M. Schanin, Soviet Physics – Technical Physics, **26**, No. 1, 120 (1981).

38 N. V. Gavrilov, Yu. E. Kreindel, E. M. Oks, P. M. Schanin, Soviet Physics – Technical Physics, **29**, No. 1, 37 (1984).

39 N. V. Gavrilov, Yu. E. Kreindel, E. M. Oks, P. M. Schanin, Soviet Physics – Technical Physics, **28**, No. 10, 1198 (1983).

40 V. L. Galanskii, Yu. E. Kreindel, E. M. Oks, P. M. Schanin, Soviet Physics – Technical Physics, **30**, No. 9, 1087 (1985).

41 I. Brown (ed.), *The Physics and Technology of Ion Sources*, 2nd edn. (Wiley-VCH, Weinheim, 2004).

42 R. Boxman, P. Martin, D. Sanders (eds.), *Handbook of Vacuum Arc Science and Technology: Fundamentals and Applications* (Noyes Publications, New Jersey, 1995).

43 V. Ya. Martens, Technical Physics, **44**, No. 7, 860 (1999).

44 A. P. Semenov, I. A. Semenova, Technical Physics, **50**, No. 4, 434 (2005).

45 A. P. Semenov, I. A. Semenova, Russian Physics Journal, **44**, No. 9, 977 (2001).

46 A. P. Semenov, Soviet Physics – Technical Physics, **32**, No. 1, 109 (1987).

47 N. V. Gavrilov, D. R. Emlin, S. P. Nikulin, Technical Physics Letters, **26**, No. 6, 498 (1999).

48 N. V. Gavrilov, S. E. Romanov, Technical Physics, **44**, No. 5, 497 (1999).

49 S. P. Nikulin, Technical Physics, **44**, No. 6, 641 (1999).

50 V. A. Gruzdev, Yu. E. Kreindel, O. E. Troyan, Soviet Physics – Technical Physics, **25**, No. 10, 1228 (1980).

51 D. M. Goebel, K. K. Jameson, R. M. Watkins, et al., Journal of Applied Physics, **98**, No. 11, 113302 (2005).

52 I. G. Mikellides, I. Katz, D. M. Goebel, et al., Journal of Applied Physics, **98**, No. 11, 113303 (2005).

53 A. Yu. Kovalenko, Yu. A. Kovalenko, Technical Physics, **48**, No. 11, 1413 (2003).

54 M. A. Vlasov, A. V. Zharinov, Yu. A. Kovalenko, Technical Physics, **46**, No. 12, 1522 (2001).

55 D. V. Mozgrin, I. K. Fetisov, G. V. Khodachenko, Plasma Physics Reports, **21**, No. 5, 400 (1995).

56 M. Yu. Kreindel, I. V. Osipov, N. G. Rempe, Soviet Physics – Technical Physics, **37**, No. 10, 1046 (1992).

57 V. F. Gruzdev, Yu. E. Kreindel, N. G. Rempe, O. E. Troyan, Instruments and Experimental Techniques, **28**, No. 1, 149 (1985).

58 W. Hartmann, G. Kirkman, V. Dominic, M. A. Gundersen, IEEE Transactions on Electron Devices, **36**, No. 4(2), 825 (1989).

59 A. P. Semenov, M. V. Mokhosoev, Soviet Physics – Doklady, **30**, No. 6, 516 (1985).